Photoinduced Oligomerization of Aqueous Pyruvic Acid

M. I. Guzmán, A. J. Colussi,* and M. R. Hoffmann

W. M. Keck Laboratories, California Institute of Technology, Pasadena, California 91125

Received: October 24, 2005; In Final Form: January 10, 2006

The 320 nm-band photodecarboxylation of aqueous pyruvic acid (PA), a representative of the α-oxocarboxylic acids widely found in the atmospheric aerosol, yields 2,3-dimethyltartaric (**A**) and 2-(3-oxobutan-2-yloxy)-2-hydroxypropanoic (**B**) acids, rather than 3-hydroxy-2-oxobutanone as previously reported. **A** and **B** are identified by liquid chromatography with UV and ESI-MS detection, complemented by collisionally induced dissociation and ^{2}H and ^{13}C isotope labeling experiments. The multifunctional ether **B** gives rise to characteristic $\delta \sim 80$ ppm ^{13}C NMR resonances. Product quantum yields are proportional to $[PA](a + [PA])^{-1}$ in the range $[PA] = 5-100$ mM. CO_2(g) release rates are halved, while **A** and **B** are suppressed by the addition of >1.5 mM TEMPO. **A** and **B** are only partially quenched in air-saturated solutions. These observations are shown to be consistent with an oligomerization process initiated by a bimolecular reaction between $^{3}PA^*$ and PA producing ketyl, $CH_3\dot{C}(OH)C(O)OH$, and acetyl, $CH_3C(O)\cdot$, radicals, rather than by the unimolecular decomposition of $^{3}PA^*$ into 1-hydroxyethylidene, $^{3}HO(CH_3)C$: $(+CO_2)$, or $[CH_3C(O)\cdot + \cdot C(O)OH]$ pairs. **A** arises from the dimerization of ketyl radicals, while **B** ensues the facile decarboxylation of the $C_8\beta$-ketoacid formed by association of acetyl radicals with the ketyl radical adduct of PA. Since the radical precursors to **A** and **B** are scavenged by O_2 with a low probability per encounter ($k_{sc} \sim 1 \times 10^6$ M^{-1} s^{-1}), PA is able to accrete into multifunctional polar species in aerated aqueous media under solar illumination.

Introduction

Pyruvic acid (PA) and other α-dicarbonyls are ubiquitous components of surface waters and the atmospheric aerosol.[1−7] They are globally produced in the photochemical degradation of the colored organic matter tinting rivers, lakes, and oceans[8] and in the atmospheric oxidation of organic gases and vapors.[9] Their fate is, however, uncertain. Species containing α-dicarbonyl moieties absorb light above ∼300 nm; i.e.,[10] they are potentially sensitive to sunlight.[11,12] In water, however, most α-dicarbonyls, with the exception of PA that substantially (∼35% at 298 K) retains its ketonic functionality, are largely hydrated into transparent *gem*-diols.[13,14] Excitation of the $n \rightarrow \pi^*$ band of aqueous PA ($\epsilon_{max} = 11.3$ M^{-1} cm^{-1} at 321 nm) induces its efficient photodecarboxylation:[15]

$$CH_3C(O)C(O)OH + h\nu \longrightarrow {}^{3}[CH_3C(O)C(O)OH]^* \longrightarrow CO_2 + \text{other products} \quad (1)$$

The identity of the other products and the mechanism of this seemingly simple process remain, however, controversial.[16,17] Early studies reported 3-hydroxy-2-oxobutanone (acetoin) is the main organic product, that pyruvate [pK_a(PA) = 2.4] is considerably more photostable than PA[15] and proposed that reaction 1 proceeds via the concerted decarboxylation of $^{3}PA^*$ into triplet 1-hydroxyethylidene [$^{3}HO(CH_3)C$:]. While a concerted process may account for the exclusive formation of acetaldehyde in the photolysis (and thermolysis) of PA in the gas phase,[15,18−21] and in the related photodecarboxylation of aqueous benzoylformic acid into benzaldehyde,[22] it is not apparent why $^{3}HO(CH_3)C$: would fail to rearrange into acetaldehyde in water as it does in the gas phase.[21] Closs and Miller (C&M)[23] interpreted their CIDNP experiments as being consistent with α-cleavage of $^{3}PA^*$ into $^{3}[CH_3C(O)\cdot \cdot COOH]$ geminate radical pairs, followed by the release of CO_2 during the subsequent reduction of PA by ·COOH. The association of the resulting ketyl and acetyl radicals would lead to 2-methyl-2-hydroxy-3-oxobutanoic acid (2-acetolactic, 2-AL), a marginally stable β-ketoacid that decarboxylates into acetoin within minutes at ambient temperature.[23,24]

A remarkable aspect of PA photochemistry is its sensitivity to the medium. Thus, PA is photostable in deaerated benzene but is photo-oxidized to peracetic acid in the presence of O_2.[25] In methanol and other hydrogen-donating solvents (even in *tert*-butyl alcohol), PA behaves as a typical ketone, being photoreduced to 2,3-dimethyltartaric and 2-methyl-2,3-dihydroxypropanoic acids without significant decarboxylation.[26] The noticeable enhancement of PA decarboxylation rates in benzene upon doping with pyridine led Davidson et al. to suggest, and explore via kinetic spectroscopy, the possibility that in inert polar solvents, such as water, the reaction actually proceeds via intermolecular photoinduced electron transfer (PET) between $^{3}PA^*$ and PA.[27−29] Since electron transfer from $^{3}PA^*$ ($E_T = 3.0$ eV)[30] to PA leading to $PA^{+\cdot}$ ($E° \sim 3.5$ V)[31] and $PA^{-\cdot}$ is thermochemically disallowed, the process likely involves proton-coupled electron transfer,[32,33] which is equivalent to H-atom transfer. A similar mechanism may apply to other carbonyls in water.[34] Bimolecular processes should be favored at the high PA concentrations prevailing in the atmospheric aerosol, over the unimolecular type 1 homolysis taking place in surface waters and, possibly, in cloud droplets.[35,36] The transition from unimolecular to bimolecular initiation mechanisms is expected to occur above ∼10 mM PA, when $^{3}PA^*$ becomes reactively

* To whom correspondence should be addressed. Telephone: (626) 395-4402. Fax: (626) 395-2940. E-mail: ajcoluss@caltech.edu.

10.1021/jp056097z CCC: $33.50
Published on Web 02/11/2006

quenched by PA ($k_Q = 2 \times 10^8$ M^{-1} s^{-1}) at rates exceeding its spontaneous decay ($k_{decay} = 2 \times 10^6$ s^{-1}).[28]

We recently reported that frozen aqueous PA glasses UV-irradiated at 77 K exhibit paramagnetic signals corresponding to distant (i.e., separated by >0.5 nm) triplet radical pairs that persist up to ~190 K.[37] The formation of distant triplet-correlated radicals in low-temperature glasses, where PA is largely associated into hydrogen-bonded cyclic dimers, is only possible via long-range (proton-coupled) electron transfer between carbonyl groups, i.e., via a bimolecular charge-transfer process related to that proposed by Davidson et al.[27−29] Here, we report that the stable products formed in the 320 nm-band photolysis of acidic, aqueous 5−100 mM PA solutions at 293 K are thermolabile C_6 and C_7 oligomers whose identification requires the use of soft analytical techniques, and propose a reaction mechanism accounting for all observations.

Experimental Section

PA (Aldrich, 0.1 M, 98.0%, bidistilled at reduced pressure) or benzoylformic acid (BF) (Aldrich, 10.0 mM, 97%, used as received) solutions in Milli-Q water (18.2 MΩ cm^{-1}) were acidified to pH 1.0 with perchloric acid (Mallinckrodt, 70% analytical reagent) prior to photolysis. Approximately 35% PA is in its photoactive keto form in water at 293 K.[13,14] These solutions were photolyzed in a sealed reactor to monitor the release of CO_2(g) via on-line absorption infrared spectrophotometry at 2349 cm^{-1}. This photochemical reactor, a cylindrical chamber provided with an axial silica finger housing the lamp (Hg Pen-Ray model CPQ 8064, emitting at 313 ± 20 nm), was coupled to an infrared cell (CaF_2 windows, 10 cm path; Bio-Rad Digilab FTS-45 FTIR spectrometer) via a circulating micropump (Schwartzer miniature pump model 135 FZ) for the continuous analysis of gas-phase products. The gas filling the entire (reactor and cell) volume was recirculated every ~4 s. PA or BF solutions (4 mL) were sparged in the reactor with ultrapure N_2 for 30 min prior to photolysis and then sealed. Solutions were magnetically stirred during photolysis. More than 98% of the CO_2 formed in reaction 1 is released into the gas phase at pH 1.0, while organic products remain in solution. Photolysis experiments were alternatively carried out on solutions contained in 3.5 mL silica UV cuvettes under continuous gas sparging, which were irradiated with light from a 1 kW high-pressure Xe−Hg lamp filtered through a 320 ± 10 nm band-pass interference filter (Oriel) and a water filter to remove unwanted infrared radiation. All experiments were performed at 293 K.

We also studied the thermal decarboxylation of aqueous 2-AL in the photochemical reactor at 293 K. 2-AL was prepared by hydrolysis of its methyl ester (Aldrich, 98%) in 0.1 M NaOH at 274 K.[24,38] A portion of this sodium 2-acetolactate solution was diluted to 2.5 mM with ultrapure water at 274 K and transferred to the photochemical reactor. After the reactor was sealed, the solution was acidified to pH 1.0 with perchloric acid injected through a septum port and rapidly thermalized at 293 K. Aqueous solutions of the radical scavenger 2,2,6,6-tetramethylpiperidin-1-oxyl (TEMPO, Aldrich, 99%, purified by vacuum sublimation) were used in some experiments. At concentrations of <4 mM, TEMPO intercepts less than 5% of the light absorbed by 0.1 M PA at ~320 nm.

Organic product analysis were performed by means of liquid chromatography at ambient temperature, using UV and electrospray ionization mass spectrometric detection (ESI-MS) (Agilent 1100 series model 1100 Series HPLC-MSD system). A ZORVAX Eclipse XDB-C18 column (3 mm × 250 mm, 5 μm, Agilent), operated under isocratic conditions [0.4 mL/min, 92.5% CHCOOH (0.1%) and 7.5% CH_3OH, from 0 to 8 min] followed by gradient elution [up to 7.5% CHCOOH (0.1%) and 92.5% CH_3OH, from 8 to 21 min], was used in these separations. The electrospray ionization inlet was set to detect negative ions in the range of 65−1000 Da.

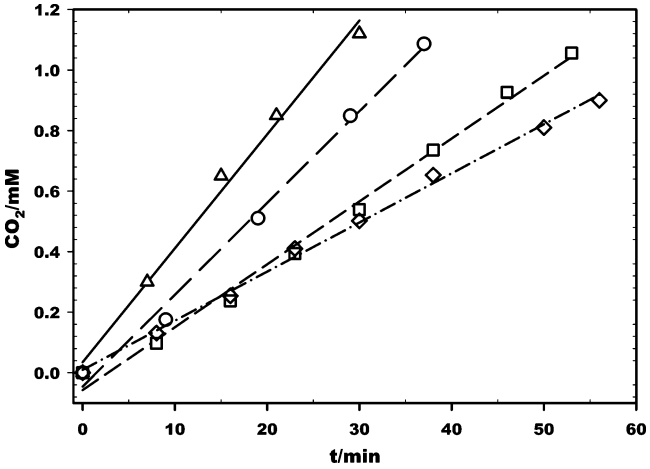

Figure 1. CO_2(g) evolution during the 313 nm photolysis of deaerated aqueous 0.1 M PA solutions at 293 K in the presence of various TEMPO initial concentrations: 0 (△), 0.50 (○), 1.36 (□), 1.71 mM (◇).

Gas chromatography−mass spectrometry analysis (Hewlett-Packard 6890 GC−5973 MSD system) were carried out using a polar polyethylene glycol (PEG) HP-INNOWax capillary column (30 m long, 0.25 mm inside diameter, coated with a 0.25 μm stationary phase film; injector at 250 °C; column temperature of 65 °C for 2 min, heating at 5 °C/min up to 100 °C and then at 25 °C/min up to 220 °C) with 70 eV electron impact ionization. Samples for analysis were prepared by mixing the analyte (250 μL) with 0.2 mM hexanol in acetonitrile as an internal standard (500 μL) and acetonitrile (250 μL).

Organic product mixtures were also analyzed by ^{13}C NMR (75 MHz Varian 300 spectrometer). [$^{13}C_3$]PA (Cambridge Isotope Laboratories, 99% $^{13}C_3$) solutions (in ultrapure water with 20% D_2O, pH 1.0) contained in sealable tubes (RotoTite, Wilmad) were degassed via freeze−thaw cycles under vacuum and then irradiated for 2 h at 293 K with the source described above (1 kW Xe−Hg lamp with a $\lambda = 320$ nm filter).

Results and Discussion

Rates of CO_2 Formation. The evolution of CO_2(g) from deaerated aqueous 0.1 M PA at pH 1.0 under continuous illumination is shown in Figure 1. Neither CO nor CH_4, which would absorb at 2169 and 3019 cm^{-1}, respectively, were formed in these experiments.[39] The CO_2 concentration values plotted in Figure 1 correspond to the number of moles of CO_2 produced divided by the volume of the aqueous PA solution (4 mL), which were obtained from integrated 2349 cm^{-1} absorption band intensities. Similar measurements of the amount of CO_2(g) released in the photolysis of deaerated BF (reaction 2):

$$C_6H_5C(O)C(O)OH + h\nu \rightarrow CO_2 + C_6H_5C(H)O \quad (2)$$

together with BF decay rates, R_{-BF}, determined by absorption spectrophotometry at 350 nm,[40] and the recently reevaluated quantum yield of reaction 2 ($\phi_2 = 0.38$),[22] lead to a ϕ_1 value of 0.39 ± 0.02, at variance with the ϕ_1 value of 0.79 previously reported.[15]

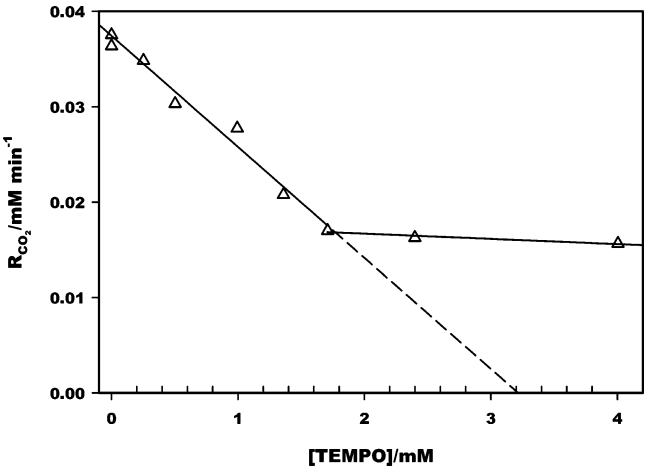

Figure 2. Rates of CO_2(g) evolution (R_{CO_2}) vs $[TEMPO]_0$ for the 313 nm photolysis of deaerated 0.1 M PA aqueous solutions at 293 K.

To test the validity of C&M's mechanism of CO_2 production in reaction 1 (reactions 3−5):

$$^3[CH_3C(O)C(O)OH]^* \rightarrow {}^3[CH_3C(O)\cdot\ \cdot C(O)OH]_{cage} \rightarrow CH_3C(O)\cdot + \cdot C(O)OH \quad (3)$$

$$CH_3C(O)C(O)OH + \cdot C(O)OH \rightarrow CO_2 + CH_3\dot{C}(OH)C(O)OH \quad (4)$$

$$CH_3\dot{C}(OH)C(O)OH + CH_3C(O)\cdot \rightarrow \text{2-AL} \rightarrow CH_3C(OH)C(O)CH_3 + CO_2 \quad (5)$$

we investigated the effect of the radical scavenger TEMPO on the initial rates of CO_2(g) evolution, R_{CO_2}, from irradiated 0.1 M PA solutions under 1 atm of N_2 at 293 K (Figures 1 and 2). R_{CO_2} was found to decrease linearly with an increase in the TEMPO initial concentration before bottoming out at $R_{CO_2,\infty} \sim 0.45R_{CO_2,0}$ for $[TEMPO]_{lim} \gtrsim 1.7$ mM (Figure 2). The endothermic decomposition of thermalized ·C(O)OH radicals

$$\cdot C(O)OH \rightarrow CO_2 + {}^{\bullet}H \quad (6)$$

with $\Delta H_6 \sim 46$ kJ/mol, $E_6 \sim 146$ kJ/mol, and $A_6 \sim 10^{13}$ s^{-1},[39] is exceedingly slow in condensed phases at 293 K. Therefore, ·C(O)OH could only generate CO_2 by reducing either PA (reaction 4) or TEMPO (reaction 7):

$$TEMPO\cdot + \cdot C(O)OH \rightarrow CO_2 + TEMPO\text{-}H \quad (7)$$

where TEMPO· explicitly depicts TEMPO as an O-centered free radical and TEMPO-H represents the hydroxylamine resulting from H-abstraction by the nitroxyl group. If reaction 4 were so fast that ∼2 mM TEMPO could not compete with 0.1 M PA toward ·C(O)OH, then TEMPO should have no effect on R_{CO_2} because, by failing to scavenge ·C(O)OH, it could not arrest the formation of the additional CO_2 produced in reaction 5. Therefore, within this scheme, the fact that TEMPO has a detrimental effect on R_{CO_2} requires that reactions 4 and 7 have competitive rates under these conditions (although we estimate, from $k_7 \sim 3 \times 10^9$ M^{-1} s^{-1} [35] and $k_4 < 1 \times 10^4$ M^{-1} s^{-1},[41] that $k_7[TEMPO]_{lim} \sim 6 \times 10^6$ s$^{-1} \gg k_4[PA] < 1 \times 10^3$ s^{-1}). Thus, by effectively scavenging ·C(O)OH via reaction 7 and, hence, by preventing the occurrence of reaction 5, TEMPO could indeed limit R_{CO_2} to approximately half the rates measured in the unscavenged system. However, if that were the case, since

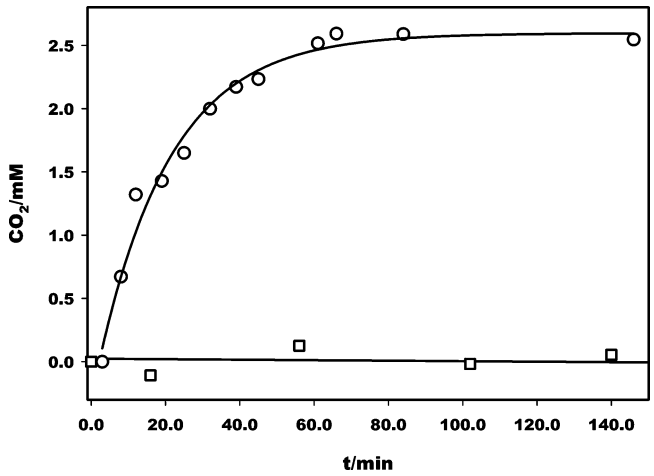

Figure 3. (□) CO_2(g) released from deaerated 0.1 M PA aqueous solutions at 293 K immediately after photolysis for 1 h. (○) CO_2(g) thermally released from aqueous 2-acetolactic acid at 293 K.

TEMPO also acts as a physical quencher of ^{3}PA* in this concentration range, as observed during the photolysis of 0.33 mM PA at >0.5 mM TEMPO,[35] $R_{CO_2,\infty}$ should tend to 0 rather than to $0.45R_{CO_2,0}$! Therefore, the fact that TEMPO fails to fully quench R_{CO_2} rules out reaction 4 as the source of CO_2 under these conditions. The results of Figure 2 seem to require instead that approximately half of the CO_2 produced in reaction 1 be formed at rates much faster than the frequency of reactive encounters with <4 mM TEMPO and the remainder via free radicals that are fully scavenged by ≳2 mM TEMPO. PA solutions previously sparged with 1 atm of O_2 release CO_2 at rates ∼25% slower than those from deaerated solutions.

Further verification of the shortcomings of C&M's proposal (reactions 3−5) is provided by the slow decarboxylation of 2-AL versus the lack of post-illumination CO_2(g) in PA photolysis (Figure 3). If 2-AL acid were the intermediate responsible for the quenchable portion of CO_2 production in the photolysis of PA (Figures 1 and 2), we should have detected the release of significant amounts of CO_2 after illumination, at variance with observations. We conclude that the CIDNP signal polarizations induced during PA photolysis in water may be consistent with the association of free radicals arising from ^{3}PA* α-cleavage (reaction 3)[23] but do not exclude other reaction pathways or provide any information about their relative contributions under specific conditions.

Organic Product Identification. A liquid chromatogram of photolyzed PA solutions is shown in Figure 4. The displayed chromatogram was obtained via ESI with negative ion mass spectral detection. A similar chromatogram is obtained by using UV detection at 254 nm. The only products formed in these experiments elute at 4.1 (**A**) and 6.9 min (**B**), which are characterized by their UV absorption (Figure 5) and mass (Figure 6) spectra. We checked that acetoin elutes at 5.3 min, and therefore, that could have been detected by UV absorption ($\lambda_{max} = 276$ nm) if it had formed. LC of PA photolysates using positive ion mass spectral detection did not reveal products other than those shown in Figure 4. The mass spectra of **A** and **B** obtained in the photolysis of [$^{13}C_3$]PA solutions in 80% H_2O/20% D_2O mixtures are shown in panels D and F of Figure 6, respectively.

It is apparent that **A** corresponds to a C_6-carboxylic acid with a molecular mass of 178 Da, because **A** is detected by negative ion mass spectrometry as its conjugated base (**A** − H)$^-$ at m/z^- 177 or 183 Da (Figure 6C,D), depending on whether it is produced in the photolysis of [$^{12}C_3$]PA or [$^{13}C_3$]PA, respectively.

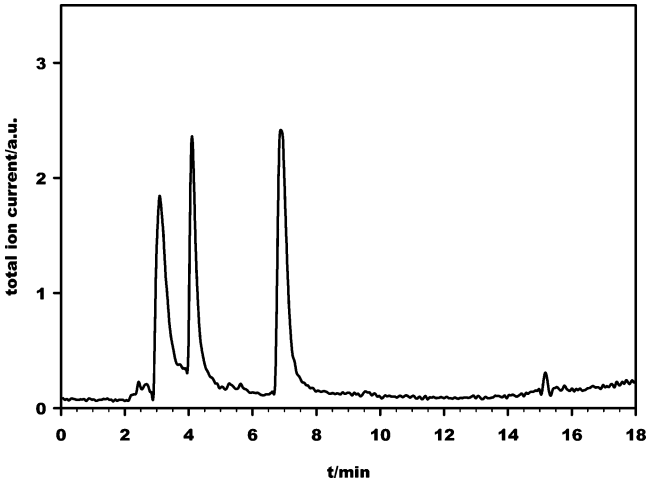

Figure 4. Liquid chromatogram of deaerated 0.1 M PA solutions after photolysis for 1 h. The species eluting at 3.1, 4.1, and 6.9 min are detected as 87, 177, and 175 Da anions, respectively, via negative ion ESI-MS.

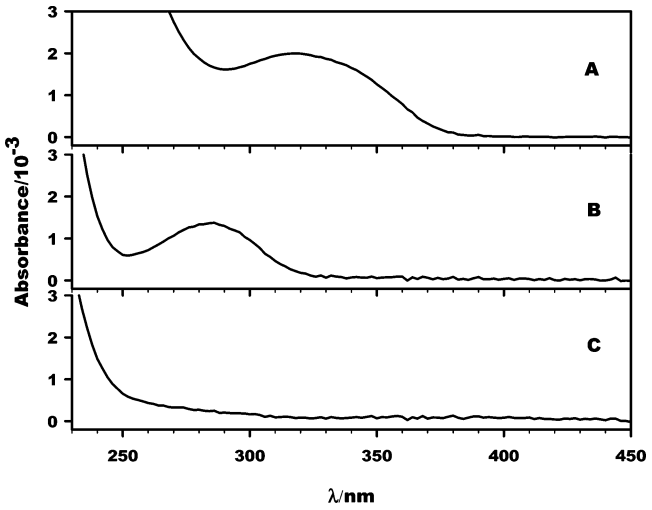

Figure 5. UV spectra of the species detected in Figure 4: spectra of the peaks eluting at 3.1 (A), 6.9 (B), and 4.1 min (C).

A lacks chromophores absorbing above ~250 nm (Figure 5C) and, furthermore, carries approximately six deuterons that are not readily exchangeable with the eluent during HPLC analysis (Figure 6D). This conclusion is based on the fact that PA exchanges all its protons, including the methyl protons, with partially deuterated water at pH 1.0 via acid-catalyzed enolization.[42] However, the labeling of its methyl protons is largely preserved during analysis using a weakly acidic eluent. Hence, the $\rho = I_{M+1}/I_M = I_{91}/I_{90} = 0.182$ ratio in the mass spectrum of [$^{13}C_3$]PA solutions prepared in partially deuterated water (Figure 6B) gauges the extent of deuteration of its methyl group. The fact that $\rho = I_{M+1}/I_M = I_{184}/I_{183} = 0.347 \sim (2 \times 0.182)$ in the mass spectrum of [$^{13}C_6$]**A** (Figure 6D) supports the presence of two methyl groups.

The collision-induced dissociation (CID) of $(\mathbf{A} - H)^-$ accelerated at 100 V leads to three prominent negatively charged fragments at m/z^- 131, 115, and 87 (Figure 6G). Dicarboxylic acids readily lose CO_2 (m/z 44) by CID unless they possess α-hydroxyls.[43,44] For example, the CID spectrum of the tartaric acid monoanion, in which both carboxyls are flanked by α-hydroxyls, only undergoes m/z 46, 62, and 90 losses. The appearance of a m/z 115 [$(\mathbf{A} - H)^- - CO_2 - H_2O$] negative fragment in the CID spectrum of **A** is actually indicative of the presence of two carboxyl groups.[45] We verified that 2,3-dihydroxy-2,3-dimethylsuccinic acid (dimethyltartaric acid), obtained by photoreduction of PA in a methanol solution,[15] elutes at 4.1 min and has a 100 V CID spectrum identical to that in Figure 6G.

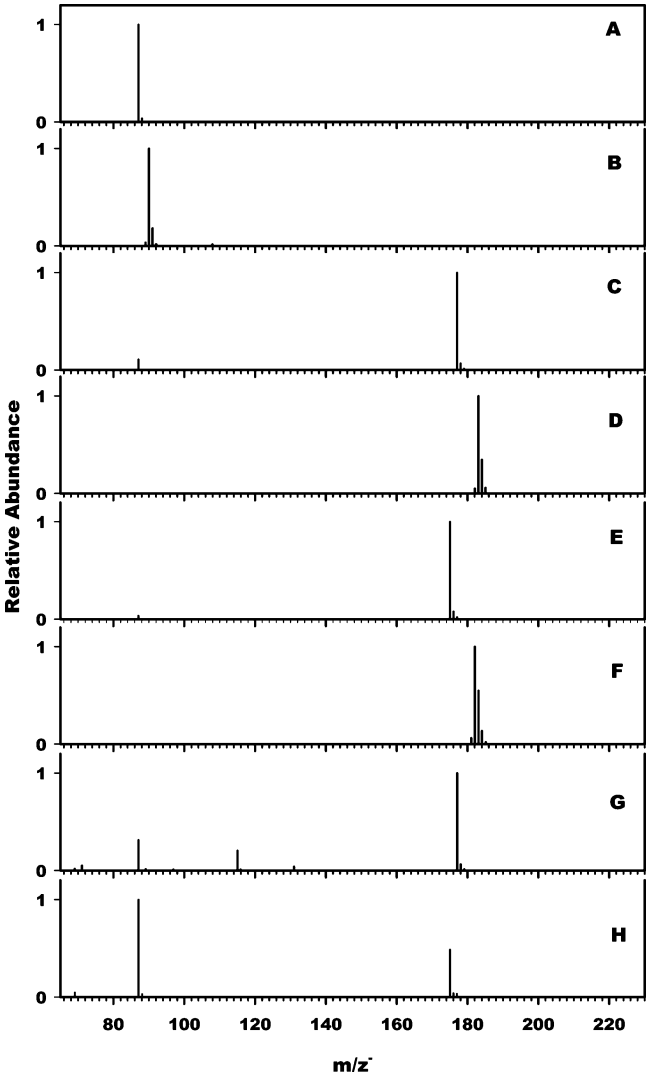

Figure 6. ESI-MS spectra of (A) PA, (B) partially deuterated [$^{13}C_3$]PA and (C) **A** (see Scheme 1), the species eluting at 4.1 min in Figure 4. (D) Same as panel C except for the photolysis of partially deuterated [$^{13}C_3$]PA. (E) **B** (see Scheme 1), the species eluting at 6.9 min in Figure 4. (F) Same as panel E except for the photolysis of partially deuterated [$^{13}C_3$]PA. (G) Fragmentation spectrum of **A** at 100 V. (H) Fragmentation spectrum of **B** at 100 V.

A similar analysis indicates that **B** (1) is a C_7-carboxylic acid with a mass of 176 Da that preserves three intact methyl groups from the PA precursor (Figure 6E,F) and (2) possesses, in contrast with **A**, a carbonyl chromophore absorbing at ~285 nm (λ_{max}) (cf. ~276 nm for acetoin) (Figure 5B). The appearance of a single fragment at m/z^- 87 [$(PA - H)^-$], i.e., the absence of a m/z^- 113 [$(PA - H)^- - CO_2 - H_2O$] fragment, in the CID mass spectrum of **B** (Figure 6H) suggests the presence of only one carboxyl group.

The 320 nm irradiation of 0.1 M [$^{13}C_3$]PA solutions for 2 h led to a mixture whose ^{13}C NMR spectrum (Figure 7C) reveals the presence of (1) carboxyl groups at $\delta = 170.4$ and 180.1 ppm [vs 167.8 ppm in keto-PA and 174.9 ppm in 2,2-dihydroxypropionic acid (DHPA), the *gem*-diol of PA; Figure 7A],[46] (2) carbonyl groups at $\delta = 204.2$ and 217.4 ppm (vs 215.5 ppm for acetoin and 201.5 ppm for PA, panels B and A of Figure 7, respectively) that confirm the absence of acetoin,

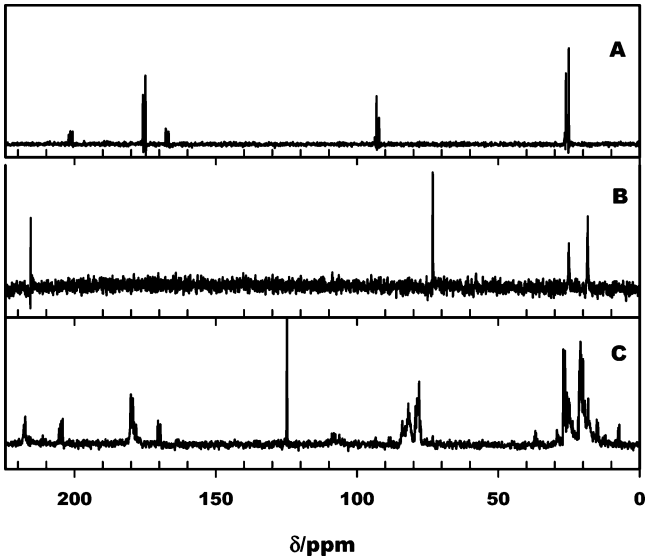

Figure 7. ^{13}C NMR spectra of (A) [$^{13}C_3$]PA, (B) 3-hydroxy-2-butanone, and (C) the photolysate of deaerated 0.1 M [$^{13}C_3$]PA after irradiation for 2 h.

and (3) a group of ether signals in the range of $\delta = 78-84$ ppm. The latter are in agreement with the resonances found in the products of the anionic polymerization of aqueous PA into linear polyethers.[47−49] The strong signal at 124.8 ppm in Figure 7C corresponds to the CO_2 product.

Effect of Radical Scavengers. The detrimental effect of radical scavengers, such as O_2 and TEMPO, on the formation of **A** and **B** confirms the involvement of free radicals in this system. Both **A** and **B** are still formed in detectable amounts in samples vigorously sparged with air, but they are effectively suppressed under continuous sparging with 1 atm of O_2 or by the addition of 2.5 mM TEMPO. From actual photochemical radical initiation rates [$R_i \sim 1.4 \times 10^{-5}$ M s^{-1} (2.5% PA losses after irradiation of deaerated 0.1 M PA for 3 min)] and by assuming diffusion-controlled radical recombination rate constants ($k_{rec} \sim 2 \times 10^9$ M^{-1} s^{-1}), we obtain steady-state radical concentrations ([X•] $\sim 6 \times 10^{-8}$ M). The observation that the yields of **A** and **B**, the products of radical recombinations (X• + X• ⟶ **A** or **B**; see Scheme 1), drop 4-fold in air ($[O_2]_{aq} = 2.8 \times 10^{-4}$ M),[50] i.e., $k_{sc}[X•][O_2]/(k_{rec}[X•]^2) \sim 3$, implies, therefore, that the relevant radicals are effectively scavenged by O_2 with k_{sc}(X•+O_2) rate constants of $\sim 1 \times 10^6$ M^{-1} s^{-1}, which are 1000 times smaller than typical diffusion-controlled k_{sc} values for the scavenging of simple C-centered radicals by O_2.[51−55] From the experiments shown in Figure 1, which involve weaker irradiances, we infer k_{sc} values for radical scavenging by TEMPO that are somewhat smaller than for O_2. The observed linear R_{CO_2} versus [TEMPO]$_0$ (Figure 2), rather than a Stern−Volmer $1/R_{CO_2}$ versus 1/[TEMPO]$_0$, dependence and the fact that the release of CO_2 is inhibited even after [CO_2] > [TEMPO]$_0$ (Figure 1) both suggest that the mechanism of inhibition involves more than simple (X• + TEMPO) recombination. Since the formation of **A** and **B** ultimately requires alkyl radical recombinations (see below), the possible competition between radical reactions with O_2 versus addition to PA does not affect the estimates of k_{sc}, given above, in our system. The fact that neither $\sim 3 \times 10^{-4}$ M O_2 nor ca. 2 mM TEMPO is able to quench ^{1,3}PA* states in the presence of 100 mM PA strongly suggests that PA itself acts as a reactive quencher.

Pyruvic Acid Concentration Effects. Previous studies of the dependence of acetyl radical formation rates on PA concentration during the photochemical decomposition of pyruvate solutions were performed in the sub-micromolar to millimolar range at pH 8.2.[35] The rate of photon absorption by PA solutions (I_a) is given by eq 8:

$$I_a = I_0[1 - \exp(-2.303\epsilon lc)] \quad (8)$$

where I_0 is the incident photon rate (in M s^{-1}), ϵ is the decadic absorption coefficient, l is the optical path length, and $c \equiv$ [PA]. When $\epsilon = \epsilon_{max} = 11.3$ M^{-1} cm^{-1} and $l = 1$ cm, I_a remains proportional to [PA]^1 at <4 mM PA. Under such conditions, therefore, the formation rates of products resulting from species generated in the unimolecular decomposition of ^{3}PA* will increase linearly with PA concentration, as observed.[35] The corresponding quantum yields (ϕ) should, of course, be independent of PA concentration.

Typical PA concentrations in atmospheric aerosols exceed, however, the range covered in ref 35. For example, Kawamura et al. report [PA]/[SO_4^{2-}] $\sim 1 \times 10^{-3}$ molar ratios in Arctic aerosols[4] and even larger ratios in urban aerosols.[5] Assuming that the upper limit to the water content of aerosol droplets is determined by the deliquescence curve of ammonium bisulfate solutions,[56] Arctic aerosol at 50% relative humidity will consist of droplets containing 0.6 g of H_2O/g of SO_4^{2-} or >20 mM PA under very acidic conditions.[57] The normalized sums of the quantum yields of formation of **A** and **B**, $\phi_A + \phi_B$, namely, the sums of their formation rates divided by I_a (from eq 8) normalized to the condition $\phi_A + \phi_B \rightarrow 1$ as [PA] $\rightarrow \infty$, measured in irradiated 5−100 mM PA solutions at pH 1, are shown in Figure 8. It is apparent that $\phi_A + \phi_B$ is not independent of [PA] above 5 mM but increases with [PA](158 + [PA])$^{-1}$. The branching ratio ϕ_B/ϕ_A also increases with [PA], as expected for the competition between the formation rates of a species (**B**) involving radical addition to a third PA versus the product (**A**) of the recombination of primary radicals. The implication is that the mechanism of photolysis of aqueous PA under these conditions is different than that in more dilute solutions and probably involves a bimolecular initiation process.

Mechanism of Reaction. The results given above can be rationalized in terms of the mechanism shown in Scheme 1. The initiation may involve photoinduced electron transfer between ^{3}PA* and ground-state PA into a bound radical ion pair,[27−29,58] as shown, or proceed via a proton-coupled electron transfer. Either pathway, whose net result is the formation of ketyl, $CH_3\dot{C}(OH)C(O)OH$(K•), and acyloxyl, $CH_3C(O)C(O)O$•, radicals in a single reactive (^{3}PA* + PA) encounter, could account for the observations presented here. Thermochemical estimates indicate, however, that PA ($\Delta_f H = 534$ kJ/mol) decompositions into [$CH_3C(O)$• + •C(O)OH] or [^{3}HO(CH_3)C: + CO_2] in the gas phase are endothermic by 304 kJ mol^{-1} and 326 kJ mol^{-1},[39,59] respectively, i.e., that both pathways require more energy than the excitation energy available to ^{3}Pa* ($E_T = 289$ kJ mol^{-1} = 30 eV), although they remain accessible to a ^{1}PA* state excited by 320 nm photons ($E_S = 372$ kJ/mol = 3.9 eV). These estimates assume that the heats of reactions involving uncharged species should not vary much from the gas phase to aqueous media. On the other hand, as indicated above, the sum of the estimated reduction potentials of the radical ions produced by direct PET between two PA molecules most likely exceeds E_T.[31] A neutral bimolecular channel [2PA ⟶ K• + $CH_3C(O)C(O)O$•, $\Delta H = 303$ kJ/mol] is also marginally accessible to triplet excitation, but the concomitant decarboxylation of $CH_3C(O)C(O)O$• into $CH_3C(O)$• and CO_2 makes the overall process quite favorable. Experiments in solvents with dissimilar polarity[60] with the direct identification of primary radical ion intermediates may resolve this issue. Regardless of

SCHEME 1

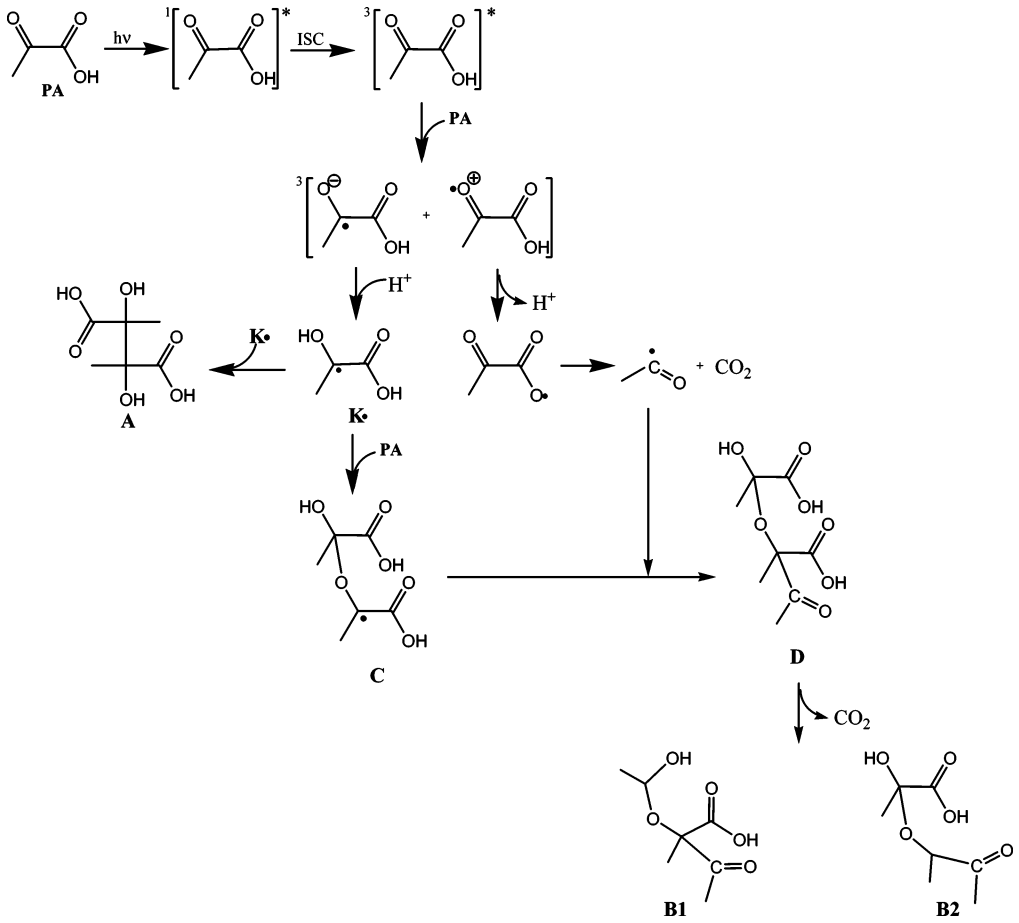

whether the $CH_3C(O)C(O)O^{\bullet}$ radical ensues after electron transfer, proton-coupled electron transfer, or H-atom transfer processes, the fact remains that its ultrafast decarboxylation ($k_9 \sim 10^{12}$ s^{-1}):[61,62]

$$CH_3C(O)C(O)O^{\bullet} \rightarrow CO_2 + CH_3CO^{\bullet} \qquad (9)$$

could not be intercepted by any of the radical scavengers used under these conditions.[63,64] The acetyl radical is rather stable to decarbonylation ($CH_3CO^{\bullet} \rightarrow CH_3^{\bullet} + CO$, $k_{dec} \sim 0.01-1$ s^{-1})[65,66] but is rapidly hydrated in aqueous solution.[67] According to Scheme 1, **A** is formed in the self-association of $K^{\bullet}$ radicals.[68−70] The formation of **B** involves the addition of $K^{\bullet}$ to PA, to either the keto form or its enol, followed by the subsequent association of **C** with the acetyl radical into the multifunctional dicarboxylic acid, **D** (220 Da). The rapid decarboxylation of **D** may proceed from the β-oxocarboxyl moiety into **B1**[71−73] or, less likely, from the α-hydroxycarboxyl moiety into **B2**. The end products of **D** decarboxylation contain (1) carbonyl groups, which give rise to the $\delta > 200$ ppm signals in Figure 7C and to the absorption spectrum of Figure 5B, and (2) ether functionalities, apparent at $\delta \sim 80$ ppm. The decarboxylation of **D** is the source of the CO_2 fraction that can be quenched by radical scavengers. **A** and **B** are thermally labile species that decompose into acetic acid, CO_2, and acetoin during conventional, high-temperature GC−MS analysis.

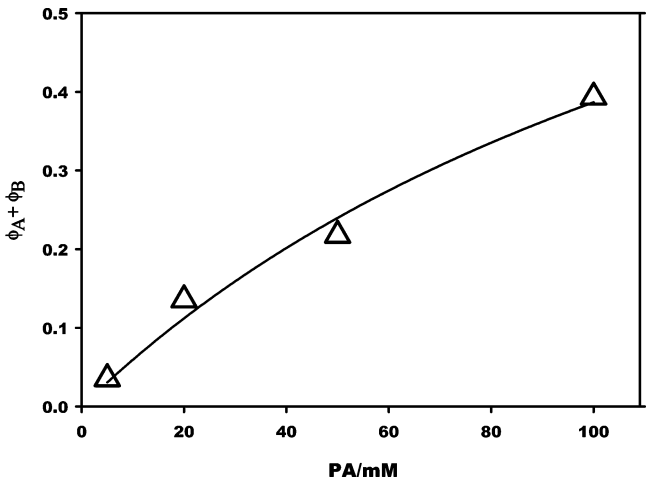

Figure 8. Sum of the apparent quantum yields of formation of **A** and **B**, $\phi_A + \phi_B$, vs [PA] in the photolysis of deaerated aqueous PA solutions at 293 K. Quantum yields normalized to the condition $(\phi_A + \phi_B) \rightarrow 1$ as [PA] $\rightarrow \infty$.

The results of Figure 8 can be analyzed in terms of a three-step mechanism:

$$PA + h\nu \rightarrow PA^* \qquad (10)$$

$$PA^* \rightarrow PA \qquad (11)$$

$$PA^* + PA \rightarrow X^{\bullet} + Y^{\bullet} \qquad (12)$$

followed by $X^{\bullet} + Y^{\bullet} \dashrightarrow \mathbf{A} + \mathbf{B}$, etc., which encapsulates the essence of Scheme 1 and the preceding discussion. At steady state, $[PA^*] = I_a(k_{11} + k_{12}[PA])^{-1}$, and the overall rate of product formation is given by $R_{12} = I_a k_{12}[PA](k_{11} + k_{12}[PA])^{-1}$, or $\phi_{A+B} = R_{12}/I_a \propto [PA](a + [PA])^{-1}$, where $a = k_{11}/k_{12}$, as observed. Reaction 11 may involve deactivation, as shown, and/or decomposition into species that cannot be converted into **A** and **B**.

The fact that the products of PA photolysis are inefficiently inhibited by paramagnetic scavengers, such as O_2 and TEMPO, is a remarkable finding because both the acetyl radical hydrate, $CH_3\dot{C}(OH)_2$, and the ketyl radical anion $K^{-}\cdot$, $CH_3\dot{C}(OH)C(O)O^{-}$,[74] are known to rapidly react with O_2: $k_{sc}[CH_3\dot{C}(OH)_2+O_2] = 7.7 \times 10^8\ M^{-1}\ s^{-1}$ [75] and $k_{sc}(K^{-}\cdot+O_2) = 2.6 \times 10^9\ M^{-1}\ s^{-1}$.[51,74] Some delocalized alkyl radicals, such as the methyl radical derived from *N*-nitrosodimethylamine ($k_{sc} = 5.3 \times 10^6\ M^{-1}\ s^{-1}$),[76] react with O_2 in water with rate constants that are considerably smaller than the diffusion-controlled limit. The apparently low scavenging efficiencies observed in this system should probably be ascribed, however, to other effects, such as radical stabilization via inter- or intramolecular hydrogen bonding or the lack of reactive pathways for the peroxyl radicals involved. For example, monofunctional ketyl peroxyl radicals readily split $HO_2\cdot$.[77] If $KO_2\cdot$ behaved similarly, **A** and **B** formation should have been suppressed in air-saturated solutions, at variance with our results. In this case, however, intramolecular hydrogen bonding is known to hinder internal rotation about the $CH_3\dot{C}(OH)-C(O)OH$ bond on the ESR time scale.[78] Intramolecular hydrogen bonding within the $[\dot{C}(OH)-C(O)]$ moiety should stabilize K•, possibly retard its association with O_2 (and/or shift the $K + O_2 \rightleftarrows KO_2\cdot$ equilibrium), and hamper elimination of $HO_2\cdot$ from $KO_2\cdot$. On the other hand, H-atom abstraction by peroxyl radicals, such as $CH_3C(OH)_2O_2\cdot$, is expected to be endothermic by more than 40 kJ/mol in the case of PA as a substrate.[79]

The apparent sluggishness of O_2 as a radical scavenger may, therefore, be actually associated with the fate of the derived alkylperoxyl radicals. Monofunctional α-hydroxyalkyl radicals react very rapidly with O_2,[80] but the scavenging of free radicals by sorbitol, a C_6 polyol, via H-atom abstraction leads to multifunctional ketyl radicals that undergo competitive cross-linking even in the presence of O_2.[81] The free radical scavenging activity of sugars[82−84] and related species may be a general phenomenon associated with the inability of polyhydroxylic alkyl radicals to propagate oxidative chains in water. Further work is underway.

Acknowledgment. This work was financed by NSF Grant ATM-0228140. This project benefited from the use of instrumentation made available by the Caltech Environmental Analysis Center. N. Dalleska provided valuable assistance with chromatographic analysis.

References and Notes

(1) Moran, M. A.; Zepp, R. G. *Limnol. Oceanogr.* **1997**, *42*, 1307.
(2) Andreae, M. O.; Talbot, R. W.; Li, S. M. *J. Geophys. Res.* **1987**, *92*, 6635.
(3) Mopper, K.; Zhou, X.; Kieber, R. J.; Sikorski, R. G.; Jones, R. D. *Nature* **1991**, *353*, 60.
(4) Kawamura, K.; Imai, Y.; Barrie, L. A. *Atmos. Environ.* **2005**, *39*, 599.
(5) Kawamura, K.; Yasui, O. *Atmos. Environ.* **2005**, *39*, 1945.
(6) Kawamura, K.; Yokoyama, K.; Fujii, Y.; Watanabe, O. *J. Geophys. Res.* **2001**, *106*, 1131.
(7) Kanakidou, M.; et al. *Atmos. Chem. Phys.* **2005**, *5*, 1053.
(8) Miller, W. M.; Zepp, R. G. *Geophys. Res. Lett.* **1995**, *22*, 417.
(9) Fisseha, R.; Dommen, J.; Sax, M.; Paulsen, D.; Kalberer, M.; Maurer, R.; Hofler, F.; Weingartner, E.; Baltensperger, U. *Anal. Chem.* **2004**, *76*, 6535.
(10) Calvert, G.; Pitts, J. N. *Photochemistry*; Wiley: New York, 1966.
(11) Klotz, B.; Graedler, F.; Sorensen, S.; Barnes, I.; Becker, K. H. *Int. J. Chem. Kinet.* **2001**, *33*, 9.
(12) Faust, B. P. K.; Rao, C.; Anastasio, C. *Atmos. Environ.* **1997**, *31*, 497.
(13) Buschmann, H. J.; Dutkiewicz, E.; Knoche, W. *Ber. Bunsen-Ges.* **1982**, *86*, 129.
(14) Buschmann, H. J.; Fuldner, H. H.; Knoche, W. *Ber. Bunsen-Ges.* **1980**, *84*, 41.
(15) Leermakers, P. A.; Vesley, G. F. *J. Am. Chem. Soc.* **1963**, *85*, 3776.
(16) Budac, D.; Wan, P. *J. Photochem. Photobiol., A* **1992**, *67*, 135.
(17) Wan, P.; Budac, D. *CRC Handbook of Organic Photochemistry and Photobiology*; CRC Press: Boca Raton, FL, 1995.
(18) Vesley, G. F.; Leermakers, P. A. *J. Phys. Chem.* **1964**, *68*, 2364.
(19) O'Neal, J. A.; Kreutz, T. G.; Flynn, G. W. *J. Chem. Phys.* **1987**, *87*, 4598.
(20) Turro, N. J.; Weiss, D. S.; Haddon, W. F.; McLafferty, F. W. *J. Am. Chem. Soc.* **1967**, *89*, 3370.
(21) Wesdemiotis, C.; McLafferty, F. W. *J. Am. Chem. Soc.* **1987**, *109*, 4760.
(22) Gorner, H.; Khun, H. J. *J. Chem. Soc., Perkin Trans. 2* **1999**, 2671.
(23) Closs, G. L.; Miller, R. J. *J. Am. Chem. Soc.* **1978**, *100*, 3483.
(24) Ronkainen, P.; Brummer, S.; Soumalainen, H. *Acta Chem. Scand.* **1970**, *24*, 3404.
(25) Sawaki, Y.; Ogata, Y. *J. Am. Chem. Soc.* **1981**, *103*, 6455.
(26) Kendall, D. S.; Leermakers, P. A. *J. Am. Chem. Soc.* **1966**, *88*, 2766.
(27) Davidson, R. S.; Goodwin, D. *J. Chem. Soc., Perkin Trans. 2* **1982**, 1559.
(28) Davidson, R. S.; Goodwin, D.; Fornier de Violet, P. *Chem. Phys. Lett.* **1981**, *78*, 471.
(29) Davidson, R. S.; Goodwin, D.; Pratt, J. E. *J. Chem. Soc., Perkin Trans. 2* **1983**, 1729.
(30) Formosinho, S. J. *J. Chem. Soc., Faraday Trans. 2* **1976**, *72*, 1313.
(31) Eberson, L. *Adv. Phys. Org. Chem.* **1982**, *18*, 79.
(32) Cai, Z.; Sevilla, M. D. *Top. Curr. Chem.* **2004**, *237*, 103.
(33) Cukier, R. I.; Nocera, D. G. *Annu. Rev. Phys. Chem.* **1998**, *49*, 337.
(34) Knoll, H.; Weidemann, F.; Henning, H. *React. Kinet. Catal. Lett.* **1987**, *36*, 411.
(35) Kieber, D. J.; Blough, N. V. *Free Radical Res. Commun.* **1990**, *10*, 109.
(36) Kieber, D. J.; Blough, N. V. *Anal. Chem.* **1990**, *62*, 2275.
(37) Guzmán, M. I.; Colussi, A. J.; Hoffmann, M. R. *J. Phys. Chem. A* **2006**, *120*, 931.
(38) Ronkainen, P.; Brummer, S.; Soumalainen, H. *Anal. Biochem.* **1970**, *34*, 101.
(39) NIST online databases. http://webbook.nist.gov/chemistry.
(40) Defoin, A.; Defoin-Straatmann, R.; Hilderbrand, K.; Bittersmann, E.; Kreft, D.; Khun, H. J. *J. Photochem.* **1986**, *33*, 237.
(41) Wagner, P. J.; Zhang, Y.; Puchalski, A. E. *J. Phys. Chem.* **1993**, *97*, 13368.
(42) Chiang, Y.; Kresge, A. J.; Pruszynski, P. *J. Am. Chem. Soc.* **1992**, *114*, 3103.
(43) Bandu, M. L.; Watkins, K. R.; Bretthauer, M. L.; Moore, C. A.; Desaire, H. *Anal. Chem.* **2004**, *76*, 1746.
(44) Qin, X. Z. *J. Mass Spectrom.* **2003**, *38*, 677.
(45) Moe, M. K. *Rapid Commun. Mass Spectrom.* **2005**, *19*, 859.
(46) Fischer, G.; Flatau, S.; Schellenberger, A.; Zschunke, A. *J. Org. Chem.* **1988**, *53*, 214.
(47) Kimura, H. *J. Polym. Sci., Part A: Polym. Chem.* **1996**, *34*, 3595.
(48) Kimura, H. *J. Polym. Sci., Part A: Polym. Chem.* **1998**, *36*, 189.
(49) Kimura, H. *Polym. Adv. Technol.* **2001**, *12*, 697.
(50) Aylward, G. H.; Findlay, T. J. V. *SI Chemical Data*; Wiley: New York, 1986.
(51) Neta, P.; Huie, R. E.; Ross, A. B. *J. Phys. Chem. Ref. Data* **1990**, *19*, 413.
(52) Font-Sanchis, E.; Aliaga, C.; Bejan, E. V.; Cornejo, R.; Scaiano, J. C. *J. Org. Chem.* **2003**, *68*, 3199.
(53) Scaiano, J. C.; Martin, A.; Yap, G. P. A.; Ingold, K. U. *Org. Lett.* **2000**, *2*, 899.
(54) Bejan, E. V.; Font-Sanchis, E.; Scaiano, J. C. *Org. Lett.* **2001**, *3*, 4059.
(55) El-Agamey, A.; McGarvey, D. J. *J. Am. Chem. Soc.* **2003**, *125*, 3330.
(56) Saxena, P.; Hildemann, L. M. *Environ. Sci. Technol.* **1997**, *31*, 3318.
(57) Jang, M.; Czoschke, N. M.; Northcross, A. L. *ChemPhysChem* **2004**, *5*, 1646.
(58) Davidson, R. S.; Goodwin, D.; Turnock, G. *Tetrahedron Lett.* **1980**, *21*, 4943.
(59) Liu, X.; Gross, M. L.; Wenthold, P. G. *J. Phys. Chem. A* **2005**, *109*, 2183.
(60) Griesbeck, A. G.; Kramer, W.; Oelgemoller, M. *Synlett* **1999**, 1169.
(61) Abel, B.; Assmann, J.; Buback, M.; Grimm, C.; Kling, M.; Schmatz, S.; Schroeder, J.; Witte, T. *J. Phys. Chem. A* **2003**, *107*, 9499.
(62) Bockman, T. M.; Hubig, S. M.; Kochi, J. K. *J. Org. Chem.* **1997**, *62*, 2210.
(63) Step, E. N.; Buchachenko, A. L.; Turro, N. J. *J. Am. Chem. Soc.* **1994**, *116*, 5462.

(64) Step, E. N.; Buchachenko, A. L.; Turro, N. J. *J. Org. Chem.* **1992**, *57*, 7018.
(65) Nakao, L. S.; Kadiiska, M. B.; Mason, R. P.; Grijalba, M. T.; Augusto, O. *Free Radical Biol. Med.* **2000**, *29*, 721.
(66) Fischer, H.; Paul, H. *Acc. Chem. Res.* **1987**, *20*, 200.
(67) Schuchmann, M. N.; von Sonntag, C. *J. Am. Chem. Soc.* **1988**, *110*, 5698.
(68) Negron-Mendoza, A.; Albarran, G. *Radiat. Phys. Chem.* **1990**, *35*, 469.
(69) Negron-Mendoza, A.; Castillo, S.; Torres, J. L.; Albarran, G. *Radiat. Phys. Chem.* **1988**, *31*, 825.
(70) Martin, C.; Huser, H.; Servat, K.; Kokoh, K. B. *Electrochim. Acta* **2005**, *50*, 2431.
(71) Guthrie, J. P. *Bioorg. Chem.* **2002**, *30*, 32.
(72) Huang, C. L.; Wu, C. C.; Lien, M. H. *J. Phys. Chem. A* **1997**, *101*, 7867.
(73) Sayre, L. M.; Jensen, F. R. *J. Org. Chem.* **1978**, *43*, 4700.
(74) Adams, G. E.; Willson, R. L. *J. Chem. Soc., Faraday Trans. 1* **1973**, *69*, 719.
(75) von Sonntag, C.; Schuchmann, M. N. *Angew. Chem., Int. Ed.* **1991**, *30*, 1229.
(76) Mezyk, S. P.; Cooper, W. J.; Madden, K. P.; Bartels, D. M. *Environ. Sci. Technol.* **2004**, *38*, 3161.
(77) Denisova, T. G.; Denisov, E. T. *Petroleum Chem.* **2005**, *45*, 26.
(78) Samuni, A.; Behar, D.; Fessenden, R. W. *J. Phys. Chem.* **1973**, *77*, 777.
(79) Colussi, A. J. *Chemical Kinetics of Small Organic Radicals*; CRC Press: Boca Raton, FL, 1988; Vol. 1.
(80) Jockusch, S.; Turro, N. J. *J. Am. Chem. Soc.* **1999**, *121*, 3921.
(81) Faraji, H.; Lindsay, R. C. *J. Agric. Food Chem.* **2005**, *53*, 736.
(82) Yadav, P.; Rao, B. S. M.; Batchelor, S. N.; O'Neill, P. *J. Phys. Chem. A* **2005**, *109*, 2039.
(83) Gillbe, C. E.; Sage, F. J.; Gutteridge, J. M. C. *Free Radical Res.* **1996**, *24*, 1.
(84) Morelli, R.; Russo-Volpe, S.; Bruno, N.; Lo Scalzo, R. *J. Agric. Food Chem.* **2003**, *51*, 7418.